

Mémoire de Maîtrise en Médecine No 334

**ANGIOGENESIS AND MICROCIRCULATION OF  
HUMAN MESOTHELIOMA XENOGRAFTS  
ASSESSED BY INTRAVITAL MICROSCOPY**

**Etudiant**

Sylvia Rwakabayiza

**Tuteur**

Dr Thorsten Krueger

Service de Chirurgie Thoracique et Vasculaire, CHUV

**Expert**

Prof. Hans Anton Lehr

Institut Universitaire de Pathologie, Lausanne

Lausanne, le 07.03.2012

## Introduction

Malignant pleural mesothelioma (MPM) is an aggressive malignant tumor whose principal risk factor is asbestos exposure. Its incidence varies worldwide and is around 20 per million in Europe (1). It is expected that this number will double within the next 20 years (2), will reach a peak in 2015-2020, and that the predicted number of deaths over the next 40 years will be of 250'000 in Europe (3), becoming a major health problem on a worldwide scale (4).

Despite different therapeutic strategies (multimodal treatment including surgery, chemotherapy and radiotherapy) (1, 5), the survival of patients suffering of MPM is still unsatisfactory. Therefore new treatment options, especially targeted therapies, are currently investigated. Antiangiogenic agents seem to be promising (4). Indeed, it has been shown that the prognosis in MPM is related to angiogenesis (6-8). High levels of VEGF and increased microvessel density are associated with poor outcome (6, 9). Furthermore, the highest VEGF levels of any solid tumor patients are found in mesothelioma patients (10, 11). Several antiangiogenic agents have already been tested *in vitro*, *in vivo*, or in clinical trials (11). To our knowledge, their effects on tumor angiogenesis and microcirculation have not yet been observed *in vivo*.

This study was undertaken in order to develop and standardize a new animal model for MPM, which may serve as tool for assessment of antivasular therapies directed against MPM. We evaluated tumor angiogenesis in human mesothelioma xenografts qualitatively and quantitatively during 14 days in a rodent model using a dorsal skinfold chamber (DSFC) technique and intravital microscopy (IVM), a recognized method for analysis of tumor architecture and vasculature (12). IVM permits repeated non-invasive microscopic studies of living tissue using trans- and epi-illumination microscopy.

Usually, the obtained images have to be analyzed using a sophisticated technical set-up in order to describe microcirculatory characteristics. In this study, our aim was to simplify the qualitative and quantitative evaluation of the microcirculation and to establish an easy and reproducible model for assessment of tumor angiogenesis in MPM. Therefore, we adapted a well-established and *simple* clinical scoring system initially developed for the assessment of microcirculatory perturbations in critical ill patients.

## **Material and Methods (Fig.1)**

### **Tumor model**

#### **a) Cells**

Human malignant mesothelioma cells (H-Meso-1, Deutsches Krebsforschungszentrum, Heidelberg, Germany) (13) were cultured and maintained in RPMI 1640 culture medium containing 10% fetal calf serum at 37°C and 5% CO<sub>2</sub> with adjunction of antibiotics (penicillin 1000 IU/ml and streptomycin 0.1mg/ml). For the preparation of the cell suspension, cells were washed twice with PBS and detached with trypsin. The cell suspension was centrifuged at 4000 rpm.

#### **b) Animal model**

Ten to fifteen weeks old nude mice (Charles River Laboratories, L'Arbresle, France; bodyweight 20 to 25g) were used in this study. The animals were kept in pathogen-free environment with free access to sterilized water and chow. All experiments were conducted in accordance with the national and institutional guidelines for the care and use of laboratory animals.

### **c) Generation of subcutaneous human mesothelioma xenografts**

Animals were anesthetized by intraperitoneal injection of ketamine and xylazine. A tumor cell suspension (0.1 ml containing  $5.0 \times 10^5$  H-meso-1 cells) was injected subcutaneously in the nude mice's neck using a 27-gauge needle and a 0.3-ml insulin syringe. Tumor growth was observed daily and the animals were sacrificed once the tumor volume reaches 1000 mm<sup>3</sup>.

### **d) Dorsal skin fold chamber (DSFC) (Fig. 1 a)**

DSFC were implanted in ten nude mice using the technique described by Lehr and al. (14) in order to expose the underlying muscle and its vasculature. 24 hours after its implantation, the chamber was cautiously examined to determine if there was not any inflammatory reaction that would have contraindicated its use in the study.

### **e) Tumor implantation in the dorsal skin fold chamber**

In five mice, a small piece (2x2x2 mm) of H-Meso-1 tumor previously generated was then placed in the center of each DSFC.

### **Intravital microscopy**

Using intravital microscopy, tumor size and microcirculatory parameters were analyzed during the observation period (14 days).

#### **a) Setup:**

A Carl Zeiss Axiovert 100 microscope was used for in-vivo observation of the dorsal skin fold chamber. A Plexiglas tube containing the mouse in a lateral decubitus position (ensuring that the chamber stays horizontal) was put under the microscope. The mouse was not anaesthetized. Trans-illumination and epi-illumination were performed according to the intended analysis.

Different objectives were used: Achroplan Carl Zeiss 2.5x/0.0075 and 4x/0.10 Plan Neofluar for a large field of view (3x3 mm for the 4x objective), and an achroplan 10x/0.25 objective for detailed observation of the vessels and capillaries.

Images and sequences were recorded through a CCD camera (EM-CCD C9100-12, 400 to 1000 nm, Hamamatsu Photonics, Solothurn, Switzerland) with the Hamamatsu HiPic version 7.0 software, giving 512x512 pixels and 16 bits grey level images. Finally, the acquired images were analyzed using Image J (NIH free software).

### **b) Tumor size**

Trans-illumination was performed every day and pictures were taken under the 2.5x objective. Tumor surface, length, and width, were measured using Carl Zeiss AxioVision Software Rel.4.6.

Estimation of the tumor volume was calculated using this formula:  $V = 1/6 \times \pi \times L \times l^2$ , where L is the length and l the width (15).

### **c) Angiography (Fig .1b)**

On D3, D7, D11, and D14 after tumor implantation, 2.5 ml of Fluorescein isothiocyanate-dextran (FITC-D, molecular weight 2000kDa), as fluorescent tracer, were injected in a suspension with phosphate buffer saline (PBS) into the lateral tail vein of mice. Epi-illumination (with excitation filter at  $470 \pm 20$  nm and emission filter at  $510 \pm 20$  nm) was performed and sequences were recorded during 20 sec under the 10x objective. Images were also taken under the 2.5x objective in order to determine tumor surface and vascularised surface using Carl Zeiss AxioVision Rel.4.6.

#### **d) Microcirculatory parameters analysis (Fig. 1 c)**

From the recorded sequences, tumor microcirculation was assessed. Three clinical scores describing microcirculation were used in this study: the De Backer's score, the microvascular flow index (MFI) and the heterogeneity index (15). A number of modifications were made to adapt these scores to the experimental model of growing human malignant mesothelioma. Four sites were recorded in each tumor, two in the periphery and two in the center. These sites were chosen in order to describe at each time point the most and the least vascularized part. To avoid overlapping of the analyzed regions, only one quarter of the image (using a 10x fold magnification) was analyzed.

The first score, the De Backer's score, contains vessel density (VD), perfused vessel density (PVD) and proportion of perfused vessels (PPV). Vessel density (VD) was calculated counting the vessels crossing three equidistant vertical and three equidistant horizontal lines drawn on the screen and dividing this number by the total length of the lines. The principle of this score is that density of vessels is proportional to the number of vessels crossing arbitrary lines. Perfused vessel density (PVD) was then calculated as follows: total number of vessels – (no flow + intermittent flow) / total length of the lines. Finally, Proportion of perfused vessels (PPV) was calculated using this formula:  $PPV = 100 \times PVD / VD$ .

For the second score, the microvascular flow index (MFI) (16-18), the screen was divided in four quadrants and the predominant type of flow in each quadrant was determined using these flows' characteristics: absent "0", intermittent "1", sluggish (continuous but very slow) "2", or normal "3". As normal flow rarely exist in tumor vessels, the most regular flow found in tumor vessels was considered as level "3". The MFI results from the average of the four quadrants.

The last score, the heterogeneity index, developed by Trzeciak and coworkers (17) was calculated taking the highest MFI of all sites minus the lowest MFI of all sites divided by the mean MFI of all sites.

Table 1 resumes all parameters assessed in this study.

**Table 1**

<b>Tumor morphology</b>	<b>Method</b>
Tumor surface (mm <sup>2</sup> )	Surface measurements using Zeiss Axiovision software (Fig 1d)
Tumor volume (mm <sup>3</sup> )	(width) <sup>2</sup> x length x $\pi/6$ (Fig 1e)
Vessel density (VD; n/mm)*	Number of vessels crossing the lines divided by the total length of the lines (typical example Fig 1h)
<b>De Backer's score (DBS)</b>	
Perfused vessel density (PVD; n/mm)*	Categorization of flow in each vessels crossing a line as "absent", "intermittent" or "continuous" flow; DBS = Total number of vessels – ("absent" + "intermittent " flow) / total length of the lines (Fig 1h)
Proportion of perfused vessels (PPV; %)*	100 × PVD/VD
<b>Microvascular Flow Index (MFI)</b>	
Microvascular Flow Index*	Determination of the predominant type of flow by eye in 4 quadrants: Flow characterized as "absent" (0), "intermittent" (1), "sluggish" (2), or "normal" (3) MFI = Mean value of 4 quadrants (Fig 1i)
Heterogeneity Index	(Highest MFI site – lowest MFI site)/mean MFI of all ROI

\*Assessment is performed separately for tumor periphery and center

## e) Statistical analysis

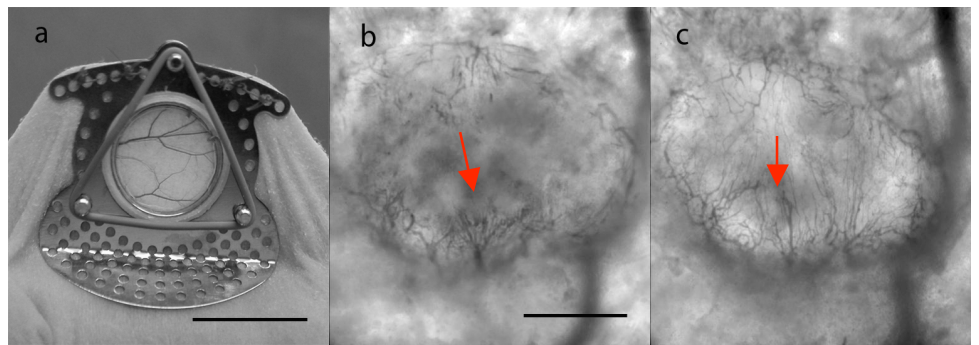
To analyze the variables "vessel density", "perfused vessel density" and "microvascular flow index", we applied the analysis of variance (ANOVA) test with repeated measures

using the software Graphpad prism 5 software package (Graphpad Software Inc, San Diego, Calif ). Tukey's HSD post hoc test was run for multiple comparisons. Data was expressed as mean  $\pm$  standard error of mean. Statistical significance was accepted at  $p < 0.05$ .

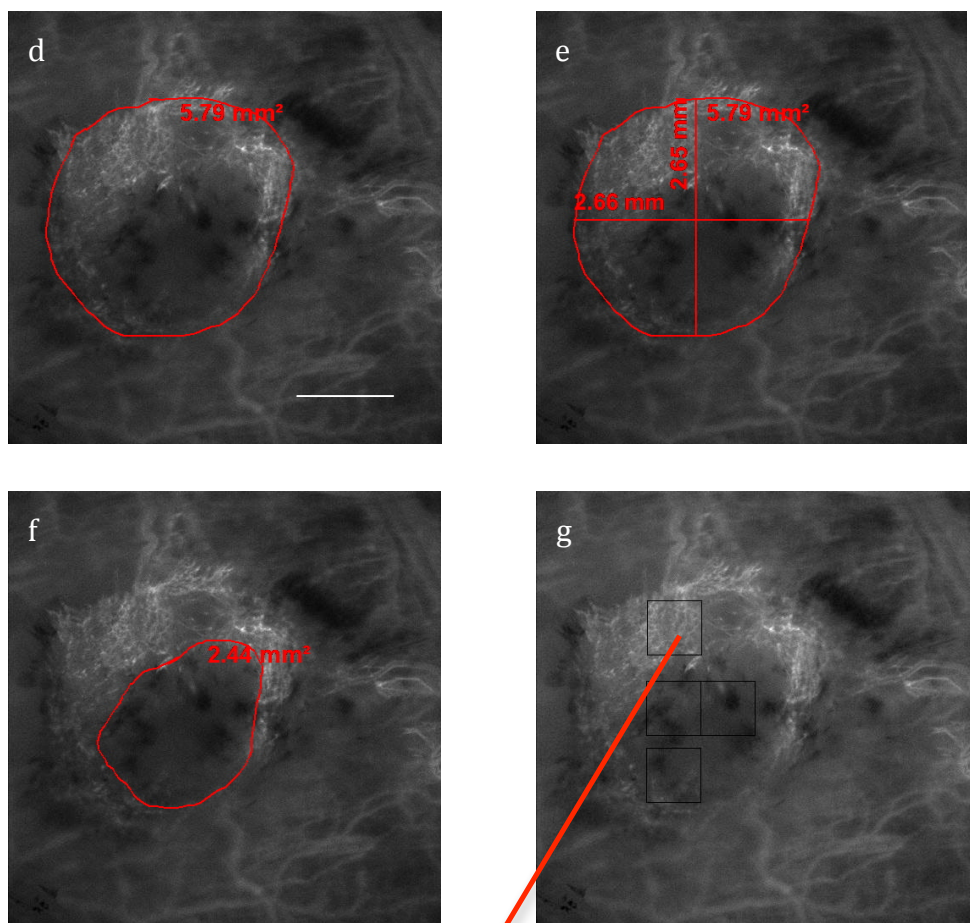


**Fig. 1**

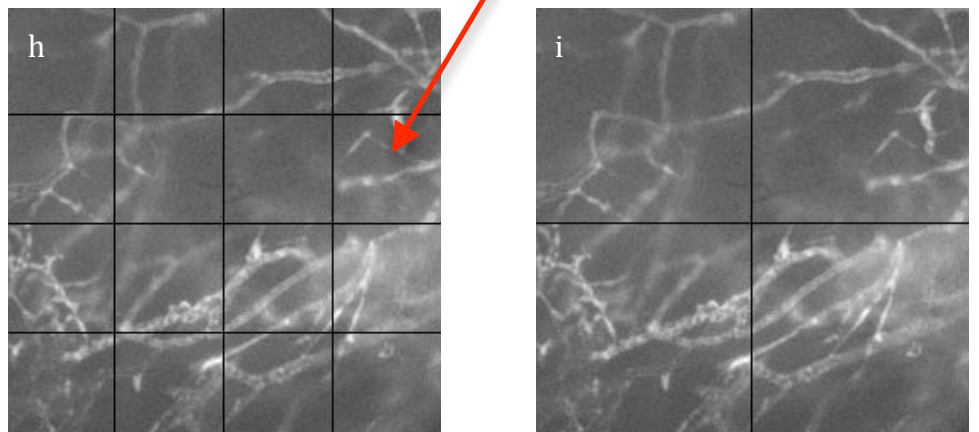
**a)** Dorsal skinfold chamber preparation in nude mice (a; bar = 10 mm) and picture of the tumor taken by IVM 7 days (b; bar = 1 mm, magnification  $\times 40$ ) and 14 days (c) after tumor implantation; flash : sprouting neovessels



**b)** Picture of the tumor taken by IVM after intravenous injection of FITC typical example (bar = 1 mm, magnification  $\times 25$ ); software based determination of surface (d), tumor dimensions (e), and non-vascularized surface (f); 4 regions of interest (ROI) (g)



**c)** Two semi-quantitative scoring systems for evaluation of microcirculation: De Backer's score (h) and Microvascular Flow Index (i) (white bar = 100  $\mu$ m, magnification  $\times 100$  )

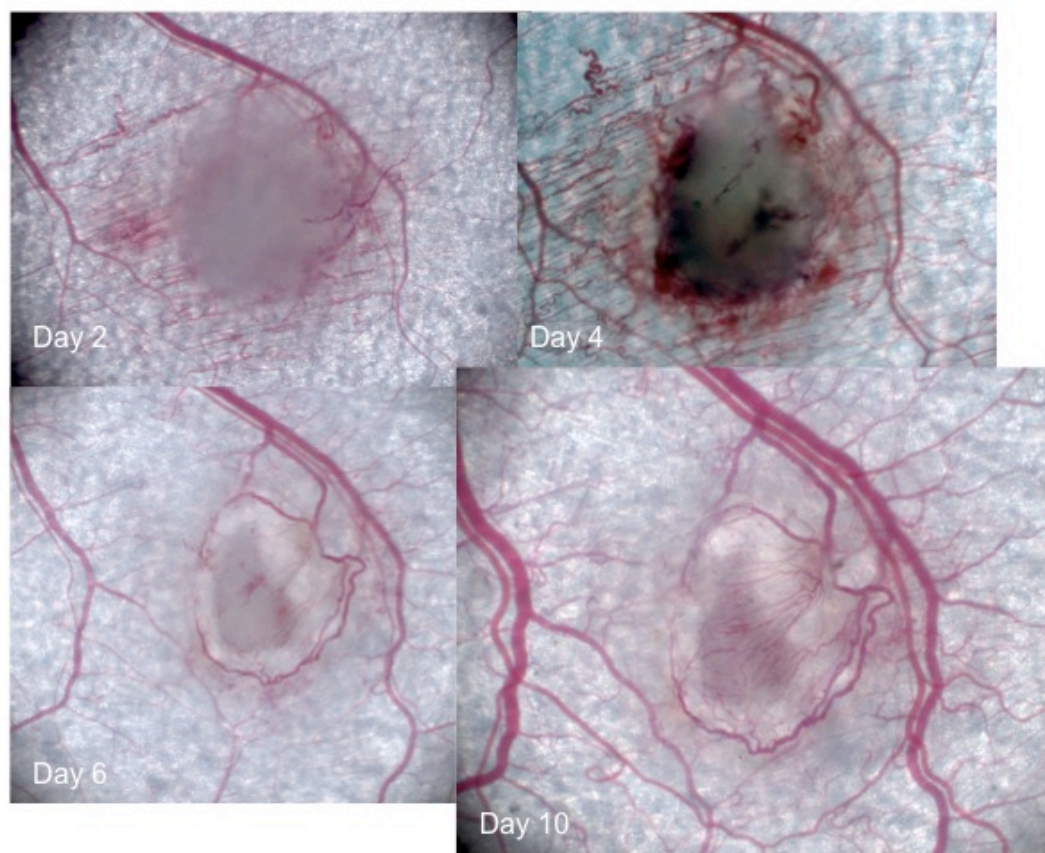


## Results

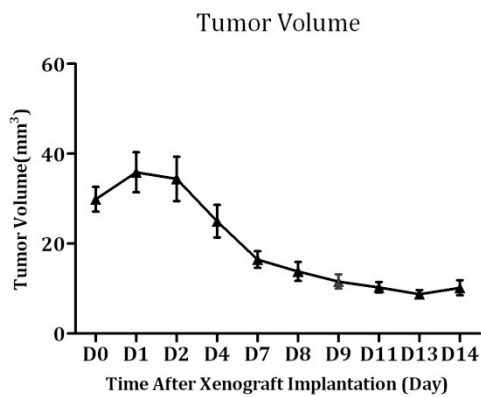
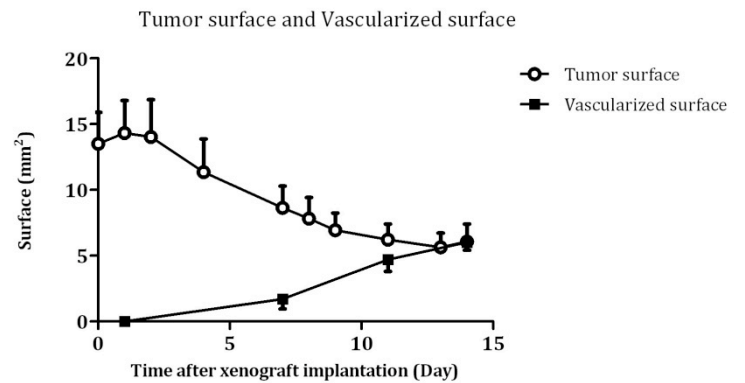
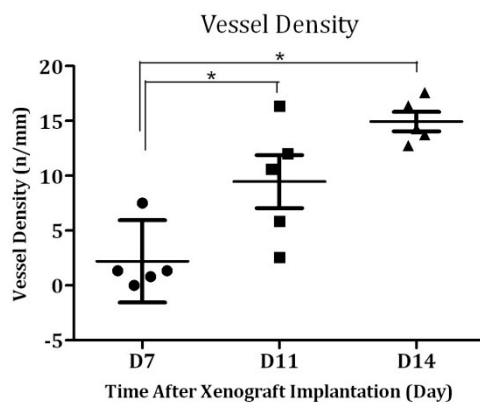
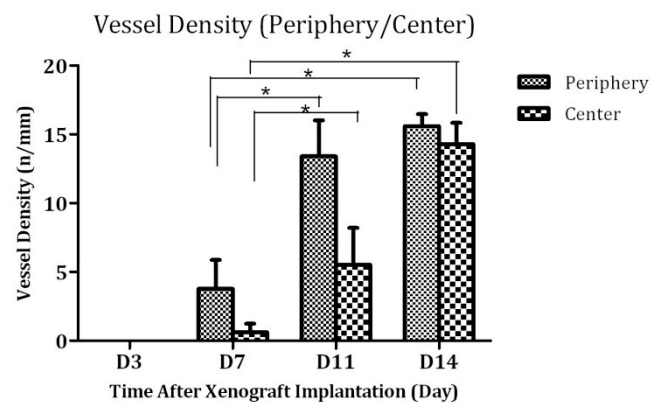
### a) Tumor morphology

The take rate of the human mesothelioma xenograft H-meso-1 in the skin fold chamber of nude mice was 100%. Three days after tumor implantation capillary sprouting was observed in the tumor periphery in 5 of 5 animals. From day 3 to 10 a progressive formation of irregularly shaped capillaries occurred, presenting an inhomogeneous blood flow. Six to 10 days after tumor grafting these newly formed vessels developed anastomoses, tumor perfusion improved with more regular flow throughout the tumor (Fig 2).

The total tumor volume and surface decreased during the observation period, while the vascularised tumor surface increased (Fig. 3). Vessel density increased progressively over time (Fig. 4; \*,  $p < 0.05$ ).



**Fig.2)** Angiogenesis, human malignant mesothelioma

**Fig. 3 a)****Fig. 3 b)****Fig. 4 a)****Fig. 4 b)**

## b) Microcirculatory parameters

Perfused vessel density and the proportion of perfused vessels increased over time (Fig. 4 and 5; \*,  $p < 0.05$ ). Microvascular flow index increased over time (Fig. 6; \*,  $p < 0.05$ ).

Tumor microcirculation is becoming more homogeneous over time (Fig. 7; \*,  $p < 0.05$ ).

**Fig. 4 a)**

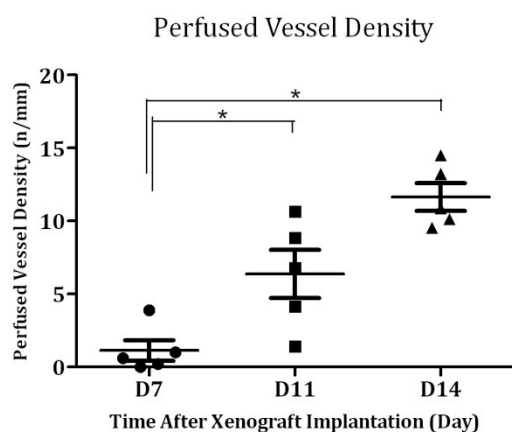


**Fig. 4 b)**

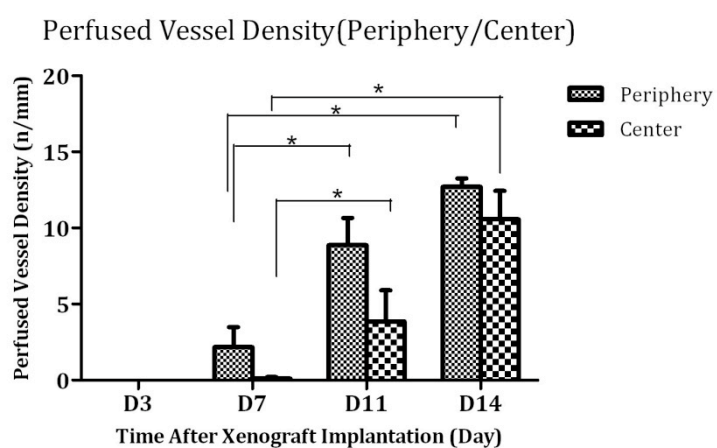


**Fig. 5**

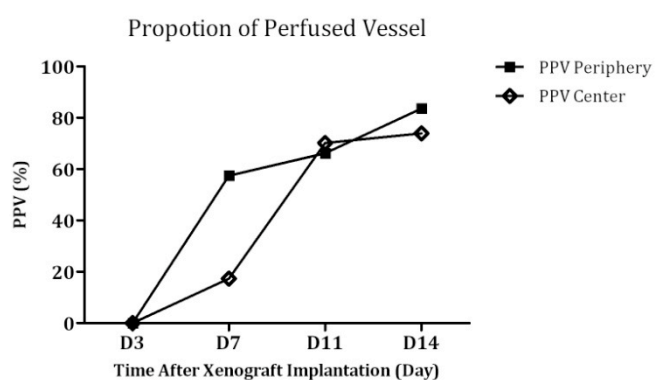


**Fig. 6 a)**

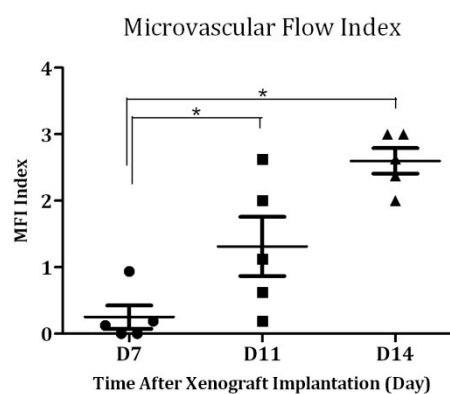


**Fig. 6 b)**

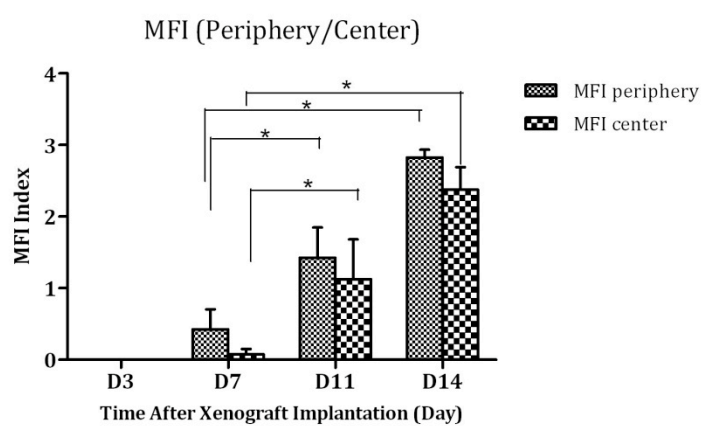
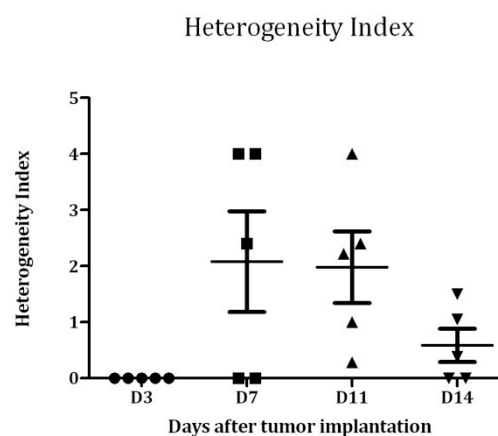


**Fig. 7**



## Discussion

The most important result of this study is that angiogenesis and microcirculation in malignant human mesothelioma can be observed *in vivo* by use of intravital microscopy and a dorsal skin fold chamber preparation in nude mice. To our knowledge, xenografting of human mesothelioma in the dorsal skin fold chamber model has not been described so far. By intravital microscopy, we observed progressive formation of neovessels during 14 days after tumor implantation, presenting an inhomogeneous blood flow. Our observation parallels different reports from the literature regarding angiogenesis observed by IVM of various solid tumors grafted in appropriate tissue preparations (12, 19-22).

The method applied in the current study for quantitative assessment of angiogenesis and microcirculation in human tumor xenografts was derived from three different clinical scoring systems for microcirculatory perturbations in critical ill patients. These clinical scores were validated by a round table conference and were published as a consensus statement by De Backer et al. (15). This consensus report describes how microcirculation should be evaluated. Importantly, the authors were able to show that the reproducibility of the defined scores is excellent, most probably due to the simplicity of the scoring system. The intra-observer variability of the De Backer's score for VD varies from 2.5% to 4.7%, for PVD from 0.9% to 4.5% and the inter-observer variability ranges from 3.0% to 6.2% and 4.1% to 10%, respectively (23). The intra-observer agreement of MFI is 85% and the inter-observer agreement is 90% (18).

Here we show that these straightforward scores can successfully be adapted to analyze *in-vivo* microcirculation in human tumor xenografts in a rodent model. However, some modifications are mandatory in order to assess at best the heterogeneity of angiogenesis

in tumor xenografts. Essentially, the number of regions to analyze has to be increased in order to take account of differences of tumor periphery and center.

In the past, several models have been used for experimental research on MPM. *In vitro* models allow to study cell morphology, proliferation, apoptosis and mutations, but only indirect means to study angiogenesis can be used, for example, by measuring VEGF levels (24, 25). A number of models consist of subcutaneous or orthotopic implantation of MPM cells in immune deficient animals or by use of syngenic malignant mesothelioma cell lines in immune competent animals (13, 25-28). They permit to test different therapeutic concepts, to evaluate survival, tumor weight and dissemination, to analyse different histopathological parameters on tumor sections, such as microvessel density. The advantages of orthotopic models compared to subcutaneous models are that tumor dissemination and selectivity of treatments can be directly observed in the native tumor's environment. The principal limitation of these models is that animals have to be sacrificed to carry out the analyses. Therefore repeated analyses over time on the same animal and tumor are impossible. As shown in our current study the main advantage of IVM and the dorsal skin fold chamber model is that it allows repeated observations over time in the same animal and tumor. However, some minor limitations need to be mentioned. The observation period is limited to 2 weeks, the skin fold chamber preparation is technically demanding and a perfect quality of the chamber without inflammation and bleeding is mandatory for valid analysis of angiogenesis, and finally FITC-dextran for angiography cannot be injected every day since otherwise its accumulation interferes with the results (19).

In conclusion, our study illustrates that angiogenesis and microcirculation in human mesothelioma xenografts can be continuously assessed *in vivo* by intravital microscopy.



The modified scoring system for assessment of tumor angiogenesis and microcirculation applied in this study is a simple, reliable and reproducible method to describe the developing neovascular network in a quantitative manner while it avoids a complicated technical setup. This model may serve as a new tool for assessment of antivascular therapies directed against MPM.

## References

1. van Meerbeeck JP, Scherpereel A, Surmont VF, Baas P. Malignant pleural mesothelioma: The standard of care and challenges for future management. *Crit Rev Oncol Hematol*. 2010. Epub 2010/05/15.
2. Stahel RA, Weder W, Lievens Y, Felip E. Malignant pleural mesothelioma: ESMO Clinical Practice Guidelines for diagnosis, treatment and follow-up. *Ann Oncol*. 2010;21 Suppl 5:v126-8. Epub 2010/06/29.
3. Robinson BW, Lake RA. Advances in malignant mesothelioma. *N Engl J Med*. 2005;353(15):1591-603. Epub 2005/10/14.
4. Greillier L, Marco S, Barlesi F. Targeted therapies in malignant pleural mesothelioma: a review of clinical studies. *Anti-cancer drugs*. 2011;22(3):199-205. Epub 2011/01/26.
5. Scherpereel A, Astoul P, Baas P, Berghmans T, Clayson H, de Vuyst P, et al. Guidelines of the European Respiratory Society and the European Society of Thoracic Surgeons for the management of malignant pleural mesothelioma. *Eur Respir J*. 2010;35(3):479-95. Epub 2009/09/01.
6. Edwards JG, Cox G, Andi A, Jones JL, Walker RA, Waller DA, et al. Angiogenesis is an independent prognostic factor in malignant mesothelioma. *Br J Cancer*. 2001;85(6):863-8. Epub 2001/09/15.
7. O'Byrne KJ, Edwards JG, Waller DA. Clinico-pathological and biological prognostic factors in pleural malignant mesothelioma. *Lung Cancer*. 2004;45 Suppl 1:S45-8. Epub 2004/07/21.
8. Kumar-Singh S, Vermeulen PB, Weyler J, Segers K, Weyn B, Van Daele A, et al. Evaluation of tumour angiogenesis as a prognostic marker in malignant mesothelioma. *J Pathol*. 1997;182(2):211-6. Epub 1997/06/01.
9. Strizzi L, Catalano A, Vianale G, Orecchia S, Casalini A, Tassi G, et al. Vascular endothelial growth factor is an autocrine growth factor in human malignant mesothelioma. *J Pathol*. 2001;193(4):468-75. Epub 2001/03/29.
10. Linder C, Linder S, Munck-Wikland E, Strander H. Independent expression of serum vascular endothelial growth factor (VEGF) and basic fibroblast growth factor (bFGF) in patients with carcinoma and sarcoma. *Anticancer research*. 1998;18(3B):2063-8. Epub 1998/07/25.

11. Zucali PA, Ceresoli GL, De Vincenzo F, Simonelli M, Lorenzi E, Gianoncelli L, et al. Advances in the biology of malignant pleural mesothelioma. *Cancer treatment reviews*. 2011;37(7):543-58. Epub 2011/02/04.
12. Jain RK, Munn LL, Fukumura D. Dissecting tumour pathophysiology using intravital microscopy. *Nat Rev Cancer*. 2002;2(4):266-76. Epub 2002/05/11.
13. Reale FR, Griffin TW, Compton JM, Graham S, Townes PL, Bogden A. Characterization of a human malignant mesothelioma cell line (H-MESO-1): a biphasic solid and ascitic tumor model. *Cancer Res*. 1987;47(12):3199-205. Epub 1987/06/15.
14. Lehr HA, Leunig M, Menger MD, Nolte D, Messmer K. Dorsal skinfold chamber technique for intravital microscopy in nude mice. *Am J Pathol*. 1993;143(4):1055-62. Epub 1993/10/01.
15. De Backer D, Hollenberg S, Boerma C, Goedhart P, Buchele G, Ospina-Tascon G, et al. How to evaluate the microcirculation: report of a round table conference. *Crit Care*. 2007;11(5):R101. Epub 2007/09/12.
16. Spronk PE, Ince C, Gardien MJ, Mathura KR, Oudemans-van Straaten HM, Zandstra DF. Nitroglycerin in septic shock after intravascular volume resuscitation. *Lancet*. 2002;360(9343):1395-6. Epub 2002/11/09.
17. Trzeciak S, Dellinger RP, Parrillo JE, Guglielmi M, Bajaj J, Abate NL, et al. Early microcirculatory perfusion derangements in patients with severe sepsis and septic shock: relationship to hemodynamics, oxygen transport, and survival. *Ann Emerg Med*. 2007;49(1):88-98, e1-2. Epub 2006/11/11.
18. Boerma EC, Mathura KR, van der Voort PH, Spronk PE, Ince C. Quantifying bedside-derived imaging of microcirculatory abnormalities in septic patients: a prospective validation study. *Crit Care*. 2005;9(6):R601-6. Epub 2005/11/11.
19. Koehl GE, Gaumann A, Geissler EK. Intravital microscopy of tumor angiogenesis and regression in the dorsal skin fold chamber: mechanistic insights and preclinical testing of therapeutic strategies. *Clin Exp Metastasis*. 2009;26(4):329-44. Epub 2009/02/05.
20. Fukumura D, Jain RK. Imaging angiogenesis and the microenvironment. *APMIS*. 2008;116(7-8):695-715. Epub 2008/10/07.
21. Hak S, Reitan NK, Haraldseth O, de Lange Davies C. Intravital microscopy in window chambers: a unique tool to study tumor angiogenesis and delivery of nanoparticles. *Angiogenesis*. 2010;13(2):113-30. Epub 2010/07/14.
22. Lunt SJ, Gray C, Reyes-Aldasoro CC, Matcher SJ, Tozer GM. Application of intravital microscopy in studies of tumor microcirculation. *J Biomed Opt*. 2010;15(1):011113. Epub 2010/03/10.
23. De Backer D, Creteur J, Preiser JC, Dubois MJ, Vincent JL. Microvascular blood flow is altered in patients with sepsis. *Am J Respir Crit Care Med*. 2002;166(1):98-104. Epub 2002/07/02.
24. Giovannetti E, Zucali PA, Assaraf YG, Leon LG, Smid K, Alecci C, et al. Preclinical emergence of vandetanib as a potent antitumour agent in mesothelioma: molecular mechanisms underlying its synergistic interaction with pemetrexed and carboplatin. *Br J Cancer*. 2011;105(10):1542-53. Epub 2011/10/06.
25. Ogino H, Yano S, Kakiuchi S, Yamada T, Ikuta K, Nakataki E, et al. Novel dual targeting strategy with vandetanib induces tumor cell apoptosis and inhibits angiogenesis in malignant pleural mesothelioma cells expressing RET oncogenic rearrangement. *Cancer letters*. 2008;265(1):55-66. Epub 2008/03/28.
26. Feins RH, Hilf R, Ross H, Gibson SL. Photodynamic therapy for human malignant mesothelioma in the nude mouse. *J Surg Res*. 1990;49(4):311-4. Epub 1990/10/01.



27. Ris HB, Giger A, Hof VI, Mettler D, Stewart JC, Althaus U, et al. Experimental assessment of photodynamic therapy with chlorins for malignant mesothelioma. *European journal of cardio-thoracic surgery : official journal of the European Association for Cardio-thoracic Surgery*. 1997;12(4):542-8. Epub 1997/11/25.
28. Tran N, Krueger T, Pan Y, Yan H, Cheng C, Altermatt HJ, et al. Correlation of photodynamic activity and fluorescence signaling for free and pegylated mTHPC in mesothelioma xenografts. *Lasers Surg Med*. 2007;39(3):237-44. Epub 2007/03/09.